

Preliminary Evaluation of a Fully-Automated Quantitative Framework for Characterizing General Breast Tissue Histology via Color Histogram and Color Texture Analysis

Brad M. Keller^a, Aimilia Gastouniotti^a, Rebecca C. Batiste^b, Despina Kontos^{a*}, Michael D. Feldman^b

^aDept. of Radiology, University of Pennsylvania, 3600 Market St. Suite 360, Philadelphia, PA 19104;

^bDept. of Pathology and Laboratory Medicine, University of Pennsylvania, Philadelphia, PA 19104

*Contact Author – em: Despina.Kontos@uphs.upenn.edu // ph: 215-746-4064

ABSTRACT

Visual characterization of histologic specimens is known to suffer from intra- and inter-observer variability. To help address this, we developed an automated framework for characterizing digitized histology specimens based on a novel application of color histogram and color texture analysis. We perform a preliminary evaluation of this framework using a set of 73 trichrome-stained, digitized slides of normal breast tissue which were visually assessed by an expert pathologist in terms of the percentage of collagenous stroma, stromal collagen density, duct-lobular unit density and the presence of elastosis. For each slide, our algorithm automatically segments the tissue region based on the lightness channel in CIE-LAB colorspace. Within each tissue region, a color histogram feature vector is extracted using a common color palette for trichrome images generated with a previously described method. Then, using a whole-slide, lattice-based methodology, color texture maps are generated using a set of color co-occurrence matrix statistics: contrast, correlation, energy and homogeneity. The extracted features sets are compared to the visually assessed tissue characteristics. Overall, the extracted texture features have high correlations to both the percentage of collagenous stroma ($r=0.95$, $p<0.001$) and duct-lobular unit density ($r=0.71$, $p<0.001$) seen in the tissue samples, and several individual features were associated with either collagen density and/or the presence of elastosis ($p\leq 0.05$). This suggests that the proposed framework has promise as a means to quantitatively extract descriptors reflecting tissue-level characteristics and thus could be useful in detecting and characterizing histological processes in digitized histology specimens.

Keywords: Quantitative Imaging, Color, Texture, Histology, Breast

Presentation Preference: Oral

1. INTRODUCTION

Visual characterization of histologic specimens is known to suffer from inter-observer and inter-laboratory variability, which may hinder the clinical utility of biomarkers derived from tissue specimens as well as the statistical power of clinical trials for biomarker discovery¹⁻³. Consequently, studies involving the characterization of histological properties of tissue samples, such as protein expression and cell density, are known to benefit from the incorporation of quantitative computer-assisted image analysis algorithms⁴⁻⁷, provided that a pathologist confirms the result⁸. As such, the development of automated tissue quantification and characterization algorithms for digital pathology data could be of great clinical utility, aiding in the reproducibility and objective quantitative characterization of histopathological tissue specimens. For example, the extracellular matrix (ECM), a critical determinant of breast density, is no longer considered an inert component in the breast microenvironment⁹, and thus the ability to quantitatively characterize collagen content and organization, a major ECM component, through immunohistochemical stains via automated color-texture algorithms could have potential utility in helping understand the breast tissue microenvironment.

In that context, this study presents a framework for the automated characterization of color content and texture in digitized histology slides. Briefly, the framework utilizes a novel application of a previously-validated, lattice-region-of-interest based algorithm for whole breast texture analysis of gray-level digital mammograms for use in color texture analysis of digitized color histology images. As a proof of concept of the potential utility of the framework in characterizing digitized histological specimens, we apply our algorithm to trichrome-stained histological samples of normal breast tissue for the purposes of characterizing collagen content. Finally, we compare our quantitative features to visual characteristics of the breast stroma assessed by an experienced breast pathologist in order to demonstrate that the

quantitative measures of color texture obtained by the algorithm reflects meaningful information of tissue composition in the image. Ultimately, we expect that application of quantitative texture measures will allow for the characterization of both total content of individual tissue-level components but also allow for the characterization of their structure and their organization. Using these tools, we will compare the strength of associations between the categorical and quantitative tissue properties and radiographic texture and density, as described above, as well as contrast the strength of the associations between the standard and computer-automated methods for describing histological tissue characteristics in order to assess the potential gain in using this system in future studies.

2. METHODS

2.1 Histology Data

In this Institutional Review Board-approved, Health Insurance Portability and Accountability Act-compliant retrospective study, formalin-fixed paraffin-embedded biopsy tissue sections from 73 women who donated normal (i.e., cancer-free) breast tissue to the Susan G. Komen for the Cure Tissue Bank (KTB) at the Indiana University Simon Cancer Center were included in the analysis. The bank and sampling procedures are approved under Indiana University's Institutional Review Board (IRB). The KTB's protocol is to acquire three tissue samples from the upper-outer quadrant of a woman's breast using 10-gauge needles and immediately process the core samples as either snap-frozen tissues or as formalin-fixed paraffin-embedded tissues¹⁰. Women with either no prior history of breast cancer or a history of unilateral breast cancer are eligible to donate to the KTB, the latter providing normal samples from their contralateral (i.e. cancer unaffected) breast. However, as women with unilateral breast cancer have 2 to 6-fold increased risk of developing contralateral breast cancer compared to the risk of the general population of women in developing a first primary cancer, the contralateral breast may reflect endogenous and/or inherent conditions which put women who developed unilateral cancer at an increased risk for cancer¹¹. As such, we restrict our analysis to those samples from women with no prior breast cancer history in order to minimize any potential biases, or the impact of other unknown confounding risk factors for cancer-affected women, for our study looking at the normal biology of breast density.

Trichrome stains were applied to the tissue sections received, which were subsequently digitized using an Aperio scanner at 20X magnification corresponding to an approximately 0.5 micron isotropic image pixel resolution. An example trichrome-stained slide is given in figure 1a. The digitized trichrome slides were visually characterized by an expert breast pathologist to assess the presence and extent of histologically relevant features. For this study, the percentage of collagenous stroma within the tissue section was scored between 0 and 100% in increments of 5%. Stromal collagen density, a measure of local collagen compactness in the stromal regions of the sample, was assessed on a 4 point scale representing low to high density patterns. The duct-lobular unit density of the tissue section was scored as a normalized continuous ratio between 0.0-1.0. Finally, the presence/absence of elastosis, clumps of elastic fibers in the stroma, was also assessed.

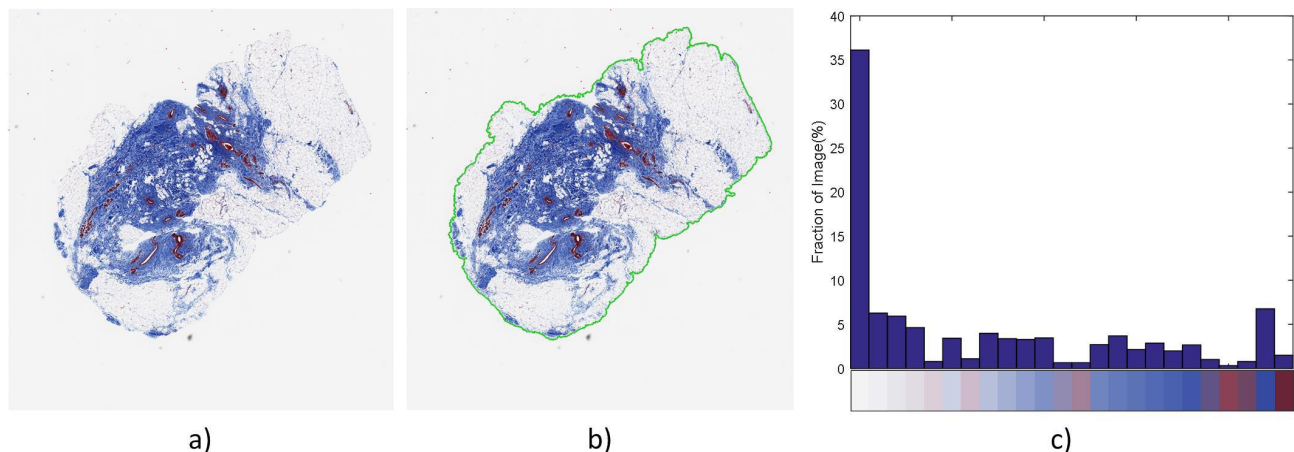


Fig. 1. Sample digitized (20X magnification), trichrome-stained breast biopsy sample of normal tissue (a), resulting automated segmentation outlined in green (b), and color content histogram for the stained tissue region with trichrome-specific color palette (c).

2.2 Automated Color Histogram and Texture Assessment from Whole-Slide Images

The first stage of the proposed tissue histology characterization framework involves automatically segmenting the regions of the slide containing the tissue specimen. Briefly, the whole-slide image digitized at 20X was first downsampled by a factor of 10 to 2X magnification for speed and memory considerations, and then converted to CIE-LAB color-space¹². The lightness (i.e., “L”) channel of the resulting images were subsequently thresholded at 95% of the maximum intensity in each specific image in order to obtain an estimate of the foreground tissue region visualized in the slide, which is predominantly of a lower intensity than the background white glass-slide region, and a morphological closing was applied to smooth out the borders. In order to capture adipose regions within the tissue, a connected-component labeling scheme was used to identify background regions fully enclosed by the foreground region identified in the previous step, which were subsequently relabeled as foreground. Lastly, to exclude small smudges and false-positive regions which may be relatively opaque versus background, foreground objects less 0.05 mm² in size were removed from the final segmentation. Figure 1b provides an example segmentation of the tissue region present in the digital slide given in figure 1a.

Within the detected tissue region, two types of features were extracted: color histogram content and color texture. First, each image was quantized so as to contain a finite number of colors, set to 24 for the purposes of this preliminary evaluation, based on a color palate generated in LAB color space and linearly ordered by lightness using a previously-described clustering approach¹³ developed for HER2/*neu* immunohistochemical staining characterization and quantification. Using the cluster-based approach, a color histogram feature vector for each slide is constructed such that the fraction of the tissue region containing each color in the palette is quantified. An example color histogram and palette is given in figure 1c. Secondly, color texture features from the quantized color images are computed using a novel application of color co-occurrence matrix (CCM) texture assessment¹⁴ to histology data in a whole-image fashion based on the lattice-texture approach proposed by Zheng et al.¹⁵, using a 100µm window-size. The CCM is similar in principal to the gray level co-occurrence matrix (GLCM)¹⁶, however, whereas the GLCM captures the frequency in which two gray-levels are adjacent in a given image, the CCM captures frequency in which specific colors are adjacent in an image at a specific angle (i.e., 0°, 45°, 90°, or 135°), which is made possible by assigning an ordinal index value to each color in the palette used to quantize the image. As such, a color co-occurrence matrix from an indexed color image can be generated using the same definitions as the GLCM such that given the indexed color image I , a prespecified offset length l , and a prespecified angle θ , the square color co-occurrence matrix C can be defined using the standard GLCM equation as given in¹⁵:

$$C(i, j) = |\{(x_1, y_1), (x_2, y_2) | I(x_1, y_1) = i, I(x_2, y_2) = j, x_2 - x_1 = l |\cos\theta|, y_2 - y_1 = l |\sin\theta|\}|, (1);$$

where x and y are the pixel coordinates and i and j are the color index labels. In this way, standard statistical measures developed to characterize the GLCM can also be directly applied to the CCM. In this study, we computed four specific texture measures developed for GLCM on the CCM matrix C in a whole-slide fashion using the proposed method:

contrast,

$$\sum_{(i,j)} |i - j|^2 \cdot C(i, j), (2);$$

correlation,

$$\sum_{(i,j)} \frac{(i - \mu_i) \cdot (j - \mu_j)}{\sigma_i \cdot \sigma_j} \cdot C(i, j), (3);$$

homogeneity,

$$\sum_{(i,j)} \frac{C(i, j)}{1 + |i - j|}, (4);$$

and energy,

$$\sum_{(i,j)} C(i, j)^2, (5);$$

where,

$$\mu_i = \sum_{(i,j)} i \cdot C(i,j), \mu_j = \sum_{(i,j)} j \cdot C(i,j), (6);$$

and

$$\sigma_i = \sum_{(i,j)} (i - \mu_i)^2 \cdot C(i,j), \sigma_j = \sum_{(i,j)} (j - \mu_j)^2 \cdot C(i,j), (7).$$

As a proof of concept for this study, we use a constant offset (i.e., l) of 3 pixels, and 4 angles for θ , namely 0° , 45° , 90° , and 135° . Examples of the contrast and homogeneity texture maps generated by the whole-slide analysis framework using the above equations for the slide given in figure 1 are provided in figure 2a and figure 2b, respectively. Finally, in order to summarize the overall color texture of each slide, the texture maps for each angle are first averaged, and then the mean texture score within the segmented tissue region is computed as has been previously suggested¹⁵.

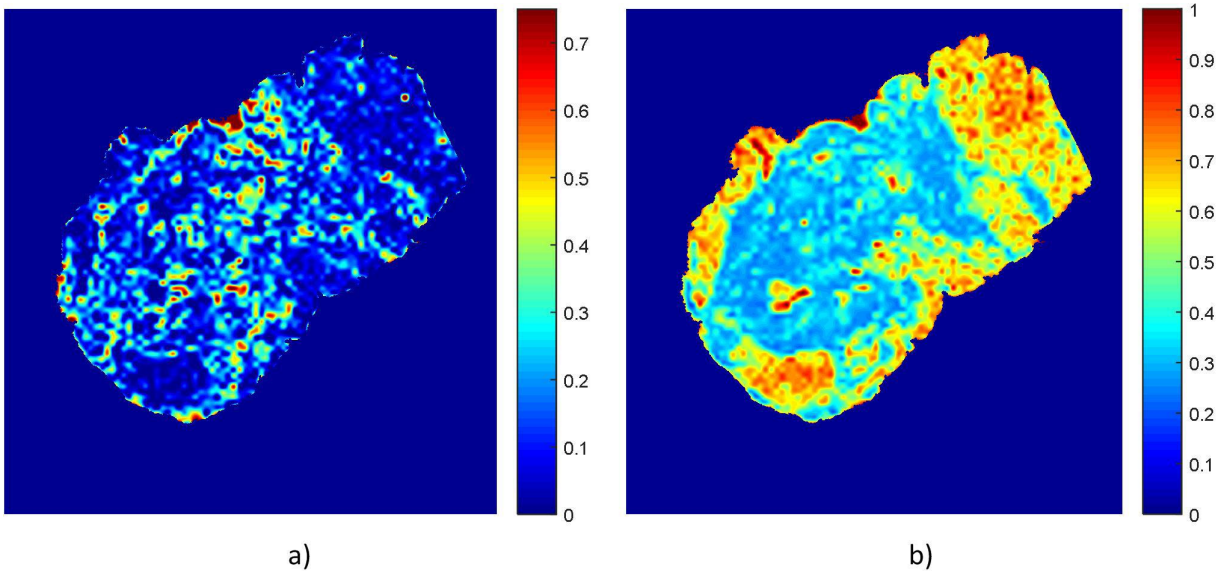


Fig. 2. Example color contrast (a) and color homogeneity (b) whole-slide texture maps of the trichrome-stained breast biopsy sample given in figure 1, with background values outside of the tissue region being set to 0 for illustration purposes.

2.3 Statistical analysis

Associations between the quantitative and pathologist-assessed measures were assessed to establish the feasibility of the automated framework presented in this work to extract clinically relevant metrics of tissue morphometry. First, all features were z-score normalized. In addition, to reduce the dimensionality of feature space, principal component analysis (PCA) was applied to the normalized color histogram feature vector, and the first 4 principal components capturing 85% of the variation were kept for subsequent analysis. Furthermore, these four color texture measures were log-transformed to improve normality. Linear regression with stepwise feature selection on the four principal components and four color-texture measures computed and Pearson correlation was used to generate algorithm-estimates of overall collagen content and duct-lobular unit density so as to determine the ability of the automated color texture features to capture histological characteristics. Analysis of Variance (ANOVA) was used to detect differences in the color texture features between the different stromal density patterns. Finally, receiver operating characteristic (ROC) curve analysis was used to determine the discriminatory capacity of the texture features to detect the presence of elastosis in the trichrome stained samples.

3. RESULTS

Linear regression showed that all four principal components of the color histogram vector along with the energy color texture feature were significantly associated ($p \leq 0.004$) with collagen content in a given trichrome slide, achieving a correlation of $r=0.95$ ($p < 0.001$; Figure 3a) between pathologist's visual assessment and the automatically quantified amount based on the color features. In addition, the first three principal components of the color histogram vector and

the energy color texture feature were also significantly associated ($p \leq 0.005$) with the density of duct-lobular units in the specimen, achieving a correlation of $r=0.71$ ($p < 0.001$; Figure 3b) between pathologist's visual assessment and the quantified amount based on the color features. ANOVA showed that the first ($p=0.001$) and third ($p=0.005$) principal components of the color histogram, as well as the color contrast ($p=0.03$), color homogeneity ($p=0.05$) and color energy ($p=0.04$) texture measures varied depending on the density of the collagen in the stroma. Finally, logistic regression showed that color homogeneity was significantly associated ($p=0.04$) with the presence of elastosis in the dataset, with an area under the ROC curve of 0.65.

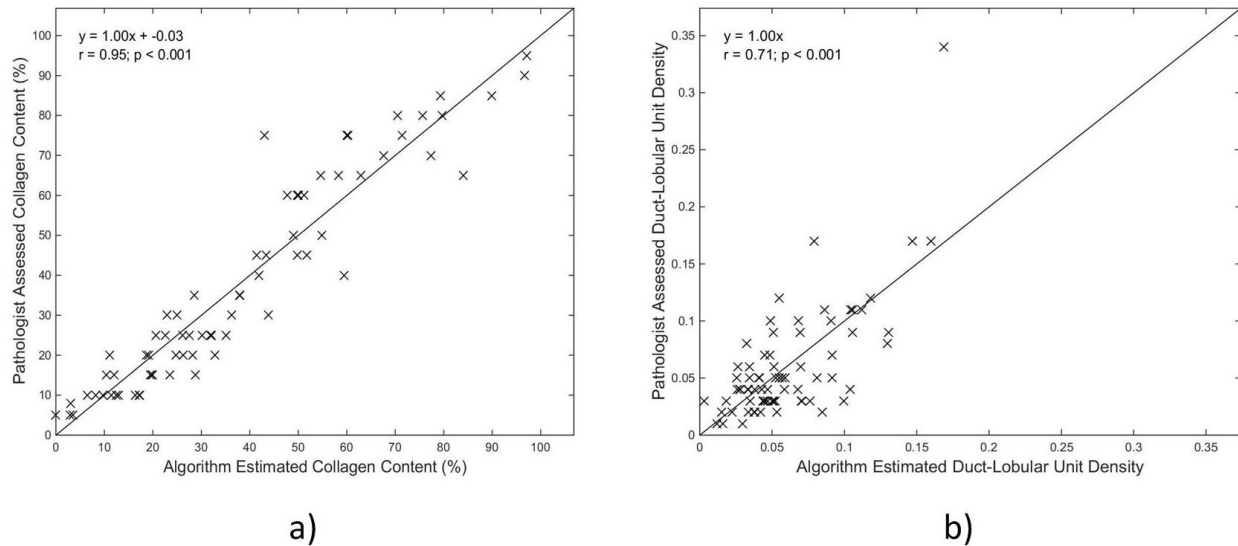


Fig. 3. Scatterplots showing algorithm estimated (x-axis) and pathologist provided scores (y-axis) of slide collagen content (a) and normalized duct-lobule unit density (b). Regression equations and lines, and Pearson correlation coefficient (r) are provided.

4. DISCUSSION

In this work, we outline a framework for fully-automated histological tissue segmentation and characterization based on novel applications of color histogram and color texture analyses. Using a dataset of 73 trichrome-stained slides containing normal breast tissue, we show that color texture feature extraction is feasible, and that extracted measures of color texture are related to visual and histologic properties seen in tissue specimens. That said, it is worth noting that we only investigate a limited subset of potential features in the present study, and only attempt to associate the texture measures with visual estimates histologic features. Furthermore, it is also worth noting that the morphologic characteristics of tissue is also important in the field of digital pathology and that this framework should be seen as a means to augment such analysis by providing additional higher-order characterization of such structure. Future work will focus on the expansion of the framework to extract additional texture features, such as additional GLCM features and run-length features, as well as exploring and optimizing the parameterization of the framework.

Overall, image texture measures are particularly useful in characterizing patterns present within biological specimens and may allow us to obtain a higher-level characterization of the spatial distribution and organization of tissue components in a given specimen. As such, color texture analysis has potentially broad-applicability as a means to quantifiably generate high-dimensional characterization of tissue samples, and we will also investigate the utility of the system in different histological stains such as hematoxylin and eosin (H&E), and for different relevant imaging tasks such as comprehensively characterizing lymphocytic infiltration or receptor staining. Ultimately, the incorporation of quantitative image texture measures will allow us to characterize patterns present within histological data, and may allow us to obtain an automated higher-level characterization of the spatial distribution and organization of tissue properties related to normal and diseased tissue structures.

5. CONCLUSION

Overall, this study presents the preliminary validation of a framework for fully-automated color-content analysis in digitized histology slides, with example applications segmentation and characterization of collagen in trichrome stained

normal breast tissue specimens based on the application of color histogram and color texture analyses. It demonstrates that automated color texture characterization is in general feasible in digitized histology images, and that extracted measures of color texture and content are associated with specific histological characteristics of the imaged tissue. Future work will seek to expand the framework to generate additional texture measures and capture morphological characteristics of the tissue specimen, validate the framework for use with additional stains such as hematoxylin and eosin (H&E) stains, study the utility of the framework in characterizing pathological processes such as tumor lesion characterization, as well as investigate the impact of various magnification scales on the analysis of specific features.

6. ACKNOWLEDGEMENTS

This research was supported by a grant from Susan G. Komen for the Cure® (PDF14299284). The authors would also like to thank Mr. Meng-kang Hsieh for assistance in processing the data utilized in this study.

7. REFERENCES

- [1] T. A. Thomson, M. M. Hayes, J. J. Spinelli *et al.*, "HER-2/neu in breast cancer: interobserver variability and performance of immunohistochemistry with 4 antibodies compared with fluorescent in situ hybridization," *Mod Pathol*, 14(11), 1079-86 (2001).
- [2] M. Mengel, R. von Wasielewski, B. Wiese *et al.*, "Inter-laboratory and inter-observer reproducibility of immunohistochemical assessment of the Ki-67 labelling index in a large multi-centre trial," *J Pathol*, 198(3), 292-9 (2002).
- [3] M. Lacroix-Triki, S. Mathoulin-Pelissier, J. P. Ghnassia *et al.*, "High inter-observer agreement in immunohistochemical evaluation of HER-2/neu expression in breast cancer: a multicentre GEFPICS study," *Eur J Cancer*, 42(17), 2946-53 (2006).
- [4] M. A. Gavrielides, B. D. Gallas, P. Lenz *et al.*, "Observer variability in the interpretation of HER2/neu immunohistochemical expression with unaided and computer-aided digital microscopy," *Arch Pathol Lab Med*, 135(2), 233-42 (2011).
- [5] T. Seidal, A. J. Balaton, and H. Battifora, "Interpretation and quantification of immunostains," *Am J Surg Pathol*, 25(9), 1204-7 (2001).
- [6] R. A. Walker, "Quantification of immunohistochemistry--issues concerning methods, utility and semiquantitative assessment I," *Histopathology*, 49(4), 406-10 (2006).
- [7] C. R. Taylor, and R. M. Levenson, "Quantification of immunohistochemistry--issues concerning methods, utility and semiquantitative assessment II," *Histopathology*, 49(4), 411-24 (2006).
- [8] A. C. Wolff, M. E. Hammond, J. N. Schwartz *et al.*, "American Society of Clinical Oncology/College of American Pathologists guideline recommendations for human epidermal growth factor receptor 2 testing in breast cancer," *Arch Pathol Lab Med*, 131(1), 18-43 (2007).
- [9] X. J. Ma, S. Dahiya, E. Richardson *et al.*, "Gene expression profiling of the tumor microenvironment during breast cancer progression," *Breast cancer research : BCR*, 11(1), R7 (2009).
- [10] M. E. Sherman, J. D. Figueroa, J. E. Henry *et al.*, "The Susan G. Komen for the Cure Tissue Bank at the IU Simon Cancer Center: a unique resource for defining the "molecular histology" of the breast," *Cancer Prev Res (Phila)*, 5(4), 528-35 (2012).
- [11] Y. Chen, W. Thompson, R. Semenciw *et al.*, "Epidemiology of contralateral breast cancer," *Cancer Epidemiol Biomarkers Prev*, 8(10), 855-61 (1999).
- [12] A. K. Jain, [Fundamentals of digital image processing] Prentice-Hall, Inc., (1989).
- [13] B. Keller, W. Chen, and M. A. Gavrielides, "Quantitative assessment and classification of tissue-based biomarker expression with color content analysis," *Arch Pathol Lab Med*, 136(5), 539-50 (2012).
- [14] V. Arvis, C. Debain, M. Berducat *et al.*, "Generalization of the cooccurrence matrix for colour images: application to colour texture classification," *Image Analysis & Stereology*, 23(1), 63-72 (2011).
- [15] Y. Zheng, B. M. Keller, S. Ray *et al.*, "Parenchymal texture analysis in digital mammography: A fully automated pipeline for breast cancer risk assessment," *Med Phys*, 42(7), 4149 (2015).
- [16] R. M. Haralick, K. Shanmugam, and I. H. Dinstein, "Textural Features for Image Classification," *Systems, Man and Cybernetics, IEEE Transactions on*, 3(6), 610-621 (1973).